Determination of Kinetic Parameters, K-m and k(cat), with a Single Experiment on a Chip

ARTICLE *in* ANALYTICAL CHEMISTRY · MAY 2009

Impact Factor: 5.64 · DOI: 10.1021/ac8020938 · Source: PubMed

4 AUTHORS, INCLUDING:

Sachin Jambovane

Pacific Northwest National Laboratory

18 PUBLICATIONS **106** CITATIONS

SEE PROFILE

Anal. Chem. **2009,** *81,* 3239–3245

Determination of Kinetic Parameters, K_m and k_{cat}, with a Single Experiment on a Chip

Sachin Jambovane,[†] Evert C. Duin,[‡] Se-Kwon Kim,[§] and Jong Wook Hong[†,*]

Materials Research and Education Center, Department of Mechanical Engineering, Auburn University, Auburn, Alabama 36849, Department of Chemistry and Biochemistry, Auburn University, Auburn, Alabama 36849, and Marine Bioprocess Research Center, Pukyong National University, Busan, 608-737, Korea

We have demonstrated a multistep enzyme reaction on a chip to determine the key kinetic parameters of enzyme reaction. We designed and fabricated a fully integrated microfluidic chip to have sample metering, mixing, and incubation functionalities. The chip generates a gradient of reagent concentrations in 11 parallel processors. We used β-galactosidase and its substrate, resorufin-β-D-galactopyranoside, as the model system of the enzyme reaction. With a single experiment on the chip, we determined the key parameters for the enzyme kinetics, K_m and k_{cat}, and evaluated the effect of inhibitor concentrations on the reaction rates. This study provides a new tool for evaluating various effectors, such as inhibitors and cofactors, on the initial rate of an enzyme reaction, and it could be applied to a comprehensive bio/chemical reaction study.

It is important to understand an enzyme reaction and its regulation mechanism not only because enzyme reactions continually influence our daily lives through biofuels and pharmaceuticals but also activities necessary to sustaining life are modulated by enzyme-catalyzed reactions.[1] Indeed, information about how different reaction conditions can influence the reaction rate, enzyme kinetics, is essential for efficient system construction in laboratories and plants.

The kinetics of enzyme is generally governed by the Michaelis−Menten equation as follows:[1–3]

$$v_0 = \frac{V_{max}[S]}{(K_m + [S])} \quad (1)$$

where v_0, [S], V_{max}, and K_m represent the initial rate of product generation, the substrate concentration, the maximum rate, and the Michaelis−Menten constant, respectively. v_0 increases as [S] increases, asymptotically approaching the maximum rate of an enzyme-mediated reaction, V_{max}. The substrate concentration at which v_0 reaches half-of V_{max} is defined as K_m and is recognized as one of the most important kinetic parameters of an enzyme. In eq 1, the v_0 of the reaction cannot be increased infinitely because of the saturation of all the active sites of the enzyme. Hence, the plot of v_0 against [S] shows the shape of a rectangular hyperbola.

At a low substrate concentration ($[S] \ll K_m$), v_0 varies linearly with the substrate concentration, which is a first-order reaction, and eq 1 is simplified to

$$v_0 = \frac{V_{max}[S]}{K_m} = \frac{k_{cat}[E][S]}{K_m} \quad (2)$$

where k_{cat} and [E] represent the turnover number and the total concentration of the enzyme, respectively. At high substrate concentrations ($[S] \gg K_m$), the rate of the reaction is independent of the substrate concentration, that is, zero-order kinetics, and eq 1 is modified to

$$v_0 = V_{max} = k_{cat}[E] \quad (3)$$

To determine the kinetic parameters of an enzyme reaction, the initial reaction rate changes as different substrate concentrations are used. Conventionally, reagents have been titrated, agitated, and analyzed in flasks or test tubes to reveal the effect of each reaction condition. In some cases, a pilot plant has been used. To obtain reliable experimental data, experienced operators must control the reactions. Moreover, it is difficult to test numerous different reaction conditions in parallel. In addition, the conventional methods require at least a few milliliters of sample for a single experiment, and this hinders the study of precious samples with limited availability. To overcome these limitations, exploiting the benefits of a microfluidic apparatus, including small sample consumption, short response times, and integration into real-time monitoring systems, is necessary.[4]

During the past decade, several microreactors have been developed to study enzyme kinetics on a chip.[5−10] The first

* To whom correspondence should be addressed. E-mail: jwhong@eng.auburn.edu.

[†] Materials Research and Education Center, Department of Mechanical Engineering, Auburn University.

[‡] Department of Chemistry and Biochemistry, Auburn University.

[§] Marine Bioprocess Research Center, Pukyong National University.

(1) Nelson, D. L.; Cox, M. M. *Lehninger Principles of Biochemistry*, 4th ed.; W. H. Freeman: New York, 2005.

(2) Segel, I. H. *Enzyme Kinetics: Behavior and Analysis of Rapid Equilibrium and Steady-State Enzyme Systems*, 1st ed.; Wiley: New York, 1975.

(3) Harvey, D. *Modern Analytical Chemistry*; McGraw-Hill: Boston, MA, 2000.

(4) Manz, A.; Harrison, D. J.; Verpoorte, E. M. J.; Fettinger, J. C.; Paulus, A.; Widmer, H. M. *J. Chromatogr.* **1992**, *593*, 253–258.

(5) Hadd, A. G.; Raymond, D. E.; Halliwell, J. W.; Jacobson, S. C.; Ramsey, J. M. *Anal. Chem.* **1997**, *69*, 3407–3412.

(6) Kerby, M.; Chien, R. L. *Electrophoresis* **2001**, *22*, 3916–3923.

(7) Song, H.; Ismagilov, R. F. *J. Am. Chem. Soc.* **2003**, *125*, 14613–14619.

(8) Duffy, D. C.; Gillis, H. L.; Lin, J.; Sheppard, N. F.; Kellogg, G. J. *Anal. Chem.* **1999**, *71*, 4669–4678.

(9) Miller, E. M.; Wheeler, A. R. *Anal. Chem.* **2008**, *80*, 1614–1619.

(10) Kang, J. H.; Park, J. K. *Sens. Actuators, B* **2005**, *107*, 980–985.

10.1021/ac8020938 CCC: $40.75
Published on Web 04/01/2009

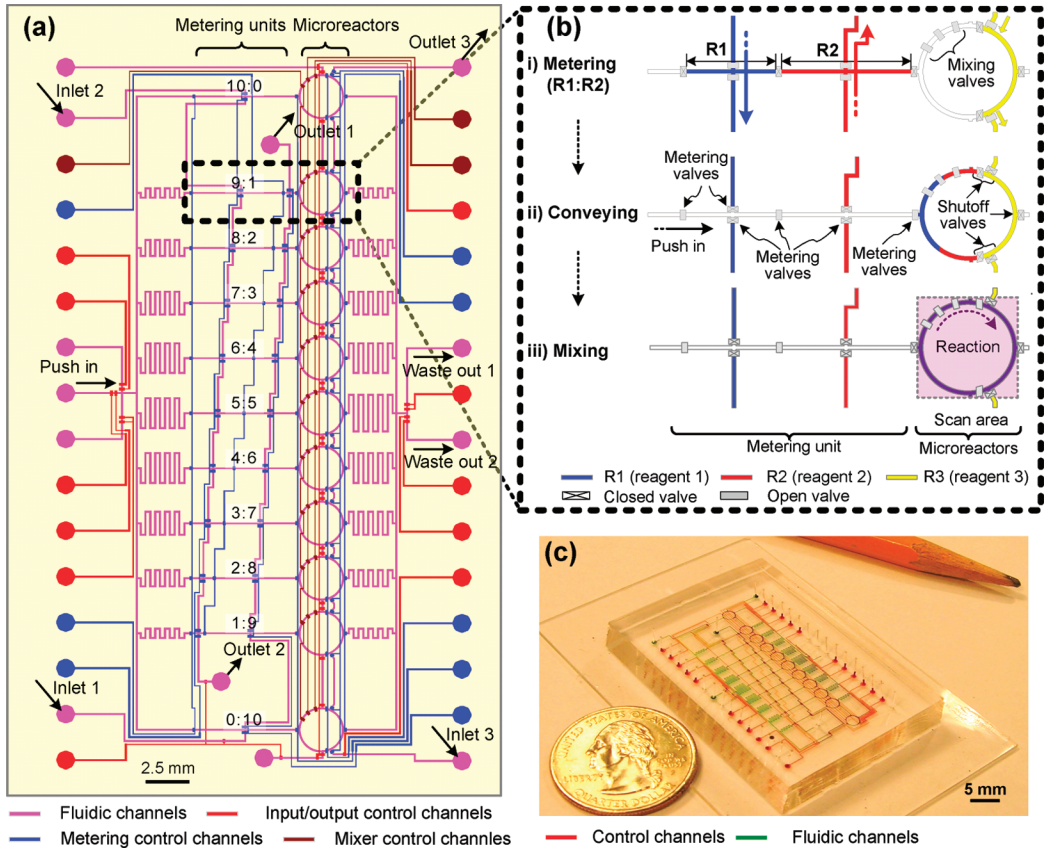

Figure 1. Integrated microfluidic system for parallel processing. (a) A configuration of the microfluidic chip. (b) Schematic process flow of (i) titering, (ii) conveying, and (iii) mixing. (c) A photograph of the microfabricated microfluidic device. With the use of the chip, 11 different reaction conditions are tested at one time.

remarkable experiment for an enzyme kinetic study was conducted by the Ramsey group with a microfabricated channel network by using an electrokinetic flow control.[5] That system showed the possibility of obtaining enzyme kinetics on a chip. Though the chip was designed to test just one reaction condition for each experiment. Because the reagents were mixed by diffusion only, mixing was relatively slow and it was difficult to get an initial reaction rate for a specified reagent concentration. In addition, electrokinetic transport, reproducibility, and long-term stability have been a major problem.[11,12] For multiple nonelectrokinetic experiments on a chip, a centrifugal microfluidic system with 48 independent microfluidic networks was devised.[8] The unique system did not have internal metering, and this led to the need for many off-chip experiments to test variations of the reaction conditions. Recently, a droplet-based microfluidic system was used to obtain kinetic parameters.[7] The droplet-based microfluidic system can perform parallel experiments without changing the geometric configuration of the microfluidic network with a highly elaborate flow controller by generating and monitoring the droplets that have different reagent concentrations.

In this paper, we demonstrate a multistep experiment on a chip with 11 parallel microfluidic processors. We borrowed the design strategy from the previous work[13,14] and extended the parallel architecture from 3 and 4 to 11 to determine the key parameters of an enzyme reaction with a single experiment without a significant increase in the number of control valves. Our chip has a metering unit and a microreactor that has mixing and incubation functionalities. To demonstrate the functionality of the present microfluidic system, we used β-galactosidase and its substrate, resorufin-β-D-galactopyranoside, as the model system. From a single experiment on a chip, we obtained the key parameters for the enzyme kinetics, K_m and k_{cat}.

MATERIALS AND METHODS

Chip Design. The microfluidic chip has 11 parallel processors, as shown in Figure 1a. The number of parallel reactions has been expanded from the previous chip design architecture.[13,14] The mixing ratio of the two reagents is determined by the ratio of the lengths of the metering channel. Figure 1b shows schematically the configuration of the single microfluidic processor and the process flow in the processor. Each processor has its own microreactor where reagents are mixed and incubated. Each microreactor has three mixing valves generating fluid flow in the microreactor and is connected with a reagent outlet port and three functional microchannels: one is a metering channel, and the others are single-reagent inlet/outlet channels which were used to simultaneously introduce a constant concentration of reagent into the 11 microreactors. The metering channel consists of two microchannels connected in a series, and each microchan-

(11) Van Orman, B. B.; Liversidge, G. G.; McIntire, G. L. *J. Microcolumn Sep.* **1990**, *2*, 176–180.
(12) Lucy, C. A.; Underhill, R. S. *Anal. Chem.* **1996**, *68*, 300–305.
(13) Hong, J. W.; Studer, V.; Hang, G.; Anderson, W. F.; Quake, S. R. *Nat. Biotechnol.* **2004**, *22*, 435–439.
(14) Marcus, J. S.; Anderson, W. F.; Quake, S. R. *Anal. Chem.* **2006**, *78*, 3084–3089.

nel can be separated flexibly by closing and opening a metering valve. The lengths of the metering channels were determined by the positions of the metering valves. Each channel is crossed with its respective reagent inlet and outlet channels. Therefore, we can simultaneously fill each of the 11 metering channels with a reagent. The reagents introduced into the metering channel and the single reagent inlet/outlet channel can be varied according to the purposes of analysis, as described in the Results and Discussion. In Figure S1a,b in the Supporting Information, a photo of the fabricated microfluidic chip with better resolution and the reagent filling scheme is shown. The flow channels are 100 μm wide and 10 ± 0.5 μm high. The width of the control channels is 50 μm except for the valve area. For the shutoff valves and mixing valves, the width is typically 200 μm. The inner diameter of each microreactor is 2.4 mm and 100 μm wide and 10 μm high, and the volume is 7.3 nL. The volume of the metered reagent is 60% of the microreactors; 40% is filled simultaneously through single-reagent inlet/outlet channels, which are connected to the 11 microreactors in series.

Chip Fabrication. We prepared mask designs by using AutoCAD software (AutoDesk Inc., San Rafael, CA) and printed them on a transparent film at 20 000 dpi (CAD/Art Services, Inc., Bandon, OR). By using photoresist-based photolithographic techniques, we fabricated molds for the two layers. At first, the positive photoresist (AZ P4620) was spin-coated onto a 4 in. silicon wafer. This was followed by UV exposure and development. For reliable opening and closing of the valves, we rounded the cross-sectional shape of the flow channels by heating the mold at 130 °C for 2 min. We made the top thick fluidic layer of the chip by pouring uncured polydimethylsiloxane (PDMS, GE RTV615; elastomer/cross-linker = 10:1) onto the fluidic layer mold to achieve a thickness of 5 mm. We made the bottom control layer of the chip by spin-coating uncured PDMS (elastomer/cross-linker = 20:1) onto the control layer mold at 2800 rpm for 1 min. The resultant thickness of the control layer membrane was 10 ± 0.5 μm. The two layers were cured for 1 h (fluidic layer) and 45 min (control layer) at 80 °C, respectively. We peeled the fluidic layer off from the mold and punched holes for the inlet/outlet ports to the flow channels through the thick layer with a 19 gauge punch (Technical Innovations, Inc., Brazoria, TX). The fluidic layer was aligned over the control layer. We bonded the two layers by baking at 80 °C for 45 min. We peeled the bonded layers off from the control layer mold and punched holes for the inlet ports to the control channels. Finally, we placed the PDMS chip on a precleaned glass slide (Fisher Scientific Pittsburgh, PA) and kept it in an oven at 80 °C for 18 h to advance curing.

Device Operation. We fabricated a microfluidic chip (Figure 1c) by using a multilayer soft lithography technique.[13,15] The microfluidic device was composed of two layers as shown in Figure S3a in the Supporting Information. When a control channel passed below a flow channel, the thin membrane between the two channels functioned as a valve. By pressurization of the control channel, the membrane was deflected and blocked the fluidic channel. By reduction of the pressure, the membrane was returned to its original shape and the fluidic channel was reopened. By using this operation principle, we controlled all the valves on a chip.

The microfluidic processors on the fabricated chip go through 3 major steps, in parallel, for a single experiment composed of 11 enzyme reactions. Figure 1b shows the step-by-step operation process in a single microfluidic processor. In addition, more detailed operation processes, including the step-by-step valve operation, are shown in Figure S3 and the supplementary movie clip in the Supporting Information. First, we infused two reagents into their respective metering channels (inlet channels 1 and 2), which are connected to the metering unit and generate the concentration gradient, and simultaneously filled the third reagent in 40% of the volume of 11 microreactors by the pressure-driven flow through the single reagent in/out the channel (inlet channel 3). In this step, we precisely controlled the pressure by using a digital flow controller as described in the Pneumatic Control section. Second, we conveyed the two reagents in the metering channel to the microreactor. In this step, the two reagents were separated from the third reagent in the microreactors using two shutoff valves to prevent unwanted initiation of the enzyme reaction. Then, we closed all the shutoff valves around the microreactor and opened the two shutoff valves separating the reagents. In this step, the sequential motion of the three mixing valves circulated and mixed the three reagents in the microreactor. After a reaction was terminated, we washed out the reaction product by introducing a washing buffer from a push-in port to the waste-out ports. In addition, selection of the inlet port for each reagent introduction was varied according to the experimental purpose. For instance, to investigate the effect of enzyme concentration on the reaction rate, we introduced an enzyme solution and an assay solution into reagent inlet channel 1 and inlet channel 2, respectively, to generate the enzyme concentration gradient. We also introduced a constant concentration of the substrate into inlet channel 3. Alternatively, to obtain the reaction rates, we switched the inlet channels for the enzyme and the substrate to inlet channel 3 and inlet channel 1, respectively.

Pneumatic Control. We operated the chip by pneumatic control. Since PDMS is permeable to gases, we filled the tubing connecting the pressure source to the shutoff valves with water to avoid bubble formation inside the flow channels. To introduce reagents into the flow channels quickly, we applied pressure, which was precisely controlled by using a flow meter (Alicat Scientific Inc., Tucson, AZ), to the backside of the reagents. The pneumatic control setup consisted of three sets of eight-channel manifolds (Fluidigm Co., San Francisco, CA) controlled by a BOB3 control board (Fluidigm Co., San Francisco, CA). A digital I/O card (National Instruments Co., Austin, TX) mounted in the computer controlled the switching of each channel of the manifolds through the BOB3 control board. We used a custom-built LabVIEW (National Instruments Co., Austin, TX) program for automatic control of the individual valves.

Enzyme Reaction. We prepared stock solutions of 261.8 mg/L of β-galactosidase (*Escherichia coli*, 465 kDa) in a reaction buffer (100 mM Tris, 2.0 mM KCl, 0.1 mM $MgCl_2$, 0.1% BSA, and 0.05% Tween 20 at pH 7.8) and 33.3 mM of resorufin-β-D-galactopyranoside (Invitrogen Inc., Carlsbad, CA) in dimethyl sulfoxide (DMSO) and stored them at −20 °C. Immediately before use, we diluted the thawed stock solutions with the reaction buffer

(15) Unger, M. A.; Chou, H. P.; Thorsen, T.; Scherer, A.; Quake, S. R. *Science* **2000**, *288*, 113–116.

solution. We purchased all chemicals except for resorufin-β-D-galactopyranoside in analytical grade from Sigma Co. (St. Louis, MO) and dissolved them in filtered Barnstead Nanopure water. To conduct the on-chip enzyme reaction, we introduced the enzyme, assay buffer, substrate, and inhibitors into each microchannel. We metered, mixed, and incubated all introduced reagents following the procedures described in the device operation section. To verify the results of the on-chip experiments, we conducted off-chip comparison experiments by using a spectrofluorometer (Perkin-Elmer L55, LAS, Boston, MA). All the conditions were the same except that milliliter volumes of cuvettes were used for the conventional experiments for the present work.

Image Acquisition and Data Processing. We used a modified biochip scanner (arrayWoRx, Applied Precision, WA) to acquire the images of the on-chip enzyme reaction (Figure S4 in the Supporting Information). We conducted multiple scans of the microfluidic chip during the course of the enzyme reactions. All the acquired images were 16-bit grayscale, the resolution was 7 800 pixels per inch (PPI), and the pixel size was 3.25 μm. To ensure enough reactor areas for data acquisition, we scanned a complete region of the 11 microreactors (38.3 mm × 3.6 mm) as shown in Figure 1b. To acquire a rectangular image (38.3 mm × 3.6 mm), we scanned a square image (1.47 mm × 1.47 mm; minimum scanning area of the scanner used in this research) 65 times (0.69 s/scan). Software (arrayWoRx 2.5 Software Suit, Applied Precision, WA) automatically converted the images to the integrated image. The total scanning time of the integrated image (38.3 mm × 3.6 mm) was approximately 45 s, as shown in Figure S5 in the Supporting Information. Within an integrated image, there is a time delay. However, by use of the integrated images, when we compared specific points or regions, there was no time delay. We used the time series analyzer of ImageJ software (http://rsb.info.nih.gov/ij/) to analyze and digitize all the fluorescence images. To evaluate the photobleaching rate of resorufin on the chip and correct the digitized data, we measured the changes in the fluorescent intensity over multiple scanning processes. We introduced resorufin (10 μM) into the 11 microreactors and measured the fluorescent intensities by collecting fluorescence signals through excitation. We observed that 0.7% of the fluorescent intensity was decreased with excitation of each scan up to 18 times (Figure S6 of the Supporting Information). The loss of fluorescent intensities was compensated by using a similar method that was developed to compensate for the photobleaching effect on a multiple scanned confocal image.[16]

RESULTS AND DISCUSSION

Chip Functionality Test and Standard Curve. To demonstrate the gradient forming functionality of the fabricated chip, we formed a gradient of resorufin on the chip by introducing 10 μM of fluorescent resorufin into reagent inlet port 1 and an assay buffer into reagent inlet ports 2 and 3 (Figure 1 and Figure S1 in the Supporting Information). A total of 11 different reagent concentrations can be generated on a chip with a complete parallel metering process. We transferred the metered reagents of resorufin and the reaction buffer and filled to 60% of the volume

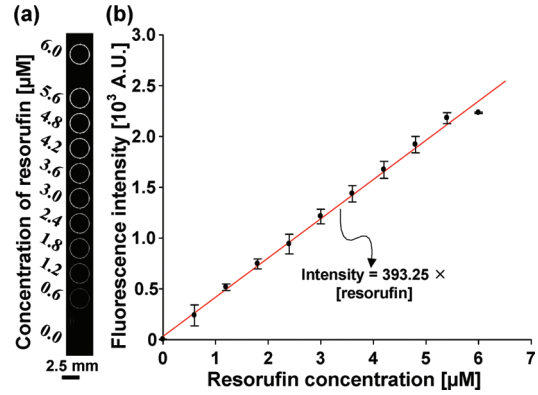

Figure 2. The relationship between the resorufin concentration and the fluorescent intensity. (a) A scanned image of the 11 microreactors showing different concentrations of the fluorescent product, resorufin. The full area of the microreactor was scanned. (b) A standard curve showing the fluorescent intensity according to the resorufin concentration increase.

of each microreactor, as shown in Figure 1b. We filled the remaining 40% with the assay buffer. Next, we mixed the three reagents, and consequently, different fluorescent intensities according to the different mixing ratios of the reagents appeared in each microreactor. We used the resultant resorufin gradient as a fluorescence standard curve for product monitoring. The product, resorufin, emits fluorescent light at 585 nm, whereas the precursor molecule resorufin-β-D-galactopyranoside does not. Thus, the increase in the fluorescent intensity can be used to monitor the rate of the product yield catalyzed by β-galactosidase when resorufin-β-D-galactopyranoside is used as a substrate. Figure 2a shows a scanned image of 11 microreactors containing different concentrations of the fluorescent resorufin, where its concentration was varied linearly from 0 to 6 μM with an increment of 0.6 μM. We digitized the quantitative information about the different concentrations of resorufin in the image and plotted the information as a standard curve, as shown in Figure 2b. We used a standard curve to quantify the concentration of product in the experiments presented hereafter. Through the on-chip parallel metering and mixing process, we demonstrated that it was possible to form a series of reagent concentrations with reagent volumes ranging from 440 pL to 4.4 nL. Compared to conventional methods,[17] the microfluidic process reduces the reaction volume by 5 orders of magnitude.

The adhesion of chemical reagents and proteins on the PDMS is well-known.[18] We also observed the adhesion of the fluorescent resorufin and the reduced linearity on the resultant standard curve. To prevent the adsorption of resorufin on the channel walls, we added 0.05% of Tween 20 and 0.1% of BSA, which are widely used as blocking reagents,[19] in the buffer solution. By using the blocking reagents, we observed a linear standard curve and enhanced consistency and reproducibility throughout the experiments.

The micromixer in each microreactor was pneumatically operated as described in the section on chip operation and showed

(16) McGrath, J. L.; Tardy, Y.; Dewey, C. F.; Meister, J. J.; Hartwig, J. H. *Biophys. J.* **1998**, *75*, 2070–2078.
(17) Huang, C. W.; Huang, S. B.; Lee, G. B. *J. Micromech. Microeng.* **2008**, *18*, 35004–35010.
(18) Toepke, M. W.; Beebe, D. J. *Lab Chip* **2006**, *6*, 1484–1486.
(19) Arenkov, P.; Kukhtin, A.; Gemmell, A.; Voloshchuk, S.; Chupeeva, V.; Mirzabekov, A. *Anal. Biochem.* **2000**, *278*, 123–131.

peristalsis similar to the movement of the gut (Figure S3b in the Supporting Information). When we operated the three consecutive valves of the micromixer in sequence, we created a unidirectional flow. By using pneumatic control, when all the valves located around each microreactor were closed, we mixed the liquid inside the microreactor. To evaluate the mixing efficiency of the micromixer, we mixed a food dye and water to visualize the mixing phenomena (Figure S3 in the Supporting Information). We captured and digitized the mixing phenomena. When the mixing was completed, the digitized value reached a constant value. The percentage of the mixing performance was increased according to the time increase. We observed 95% and 99.9% mixing performance in 13.8 and 24.6 s, respectively, under the conditions of our experiments. The average speed was 1.4 ± 0.1 mm/s, and the number of circulation for achieving 99.9% mixing performance was 4.4 ± 0.4.

Optimization of Enzyme Concentration. The kinetic study of an enzyme starts to determine the length of a linear region in a product formation as a function of time.[2] When the product is overaccumulated, the relationship between the enzyme concentration, [E], and initial rate, v_0, becomes nonlinear. Consequently, the rate of product formation is too fast, and the range of linearity is short. Then, it is difficult to obtain a sufficient number of data points to calculate v_0. Therefore, [E] of the enzyme reaction needs to be adjusted to control the rate of the product formation and to obtain sufficiently long linearity. To adjust the enzyme concentrations, we formed the concentration gradient of β-galactosidase ranging from 27.9 to 279 μg/L, with an increment of 27.9 μg/L by introducing 465 μg/L of β-galactosidase and assay buffer into reagent inlet ports 1 and 2, respectively. Substrate (333.3 μM) was also introduced into the reagent inlet port 3 to supply 133.3 μM of substrate to each reaction. Figure 3a shows the full progress curve of the product formation with the increase in enzyme concentration. The changes in v_0 as a function of [E] are also plotted in Figure 3b. We observed that the enzyme reactions with [E] up to 139.5 μg/L did not reach a plateau in 110 min of reaction time. Hence, we used [E] of less than 139.5 μg/L and data points up to 600 s in the experiments presented hereafter.

Effects of Inhibitors. The response of the enzyme activity to total inhibitor concentration, [I], is important for understanding the regulation mechanism.[20,21] We evaluated the effect of [I] on v_0 with a single experiment on a chip. For this experiment, we used phenylethyl β-D-thiogalactoside (PETG) and lactose as competitive inhibitors of β-galactosidase. To produce a series of reaction conditions, we introduced 40 μM of PETG and 33.3 mM of lactose in assay buffer containing 139.5 μg/L of β-galactosidase into reagent inlet port 1 and introduced assay buffer containing 139.5 μg/L of β-galactosidase into reagent inlet port 2. We introduced 333 μM of substrate into reagent inlet port 3 to supply a constant concentration of substrate. The resultant concentration ranges of the inhibitors were 2.4−24 μM for PETG and 2−20 mM for lactose. We used the enzyme concentration (83.7 μg/L) and the substrate concentration (133.3 μM) as the final concentrations for the experiments.

(20) Segel, I. *Enzyme Kinetics*; Wiley: New York, 1993.
(21) Copeland, R. A. *Evaluation of Enzyme Inhibitors in Drug Discovery: A Guide for Medicinal Chemists and Pharmacologists*; Wiley: New York, 2005.

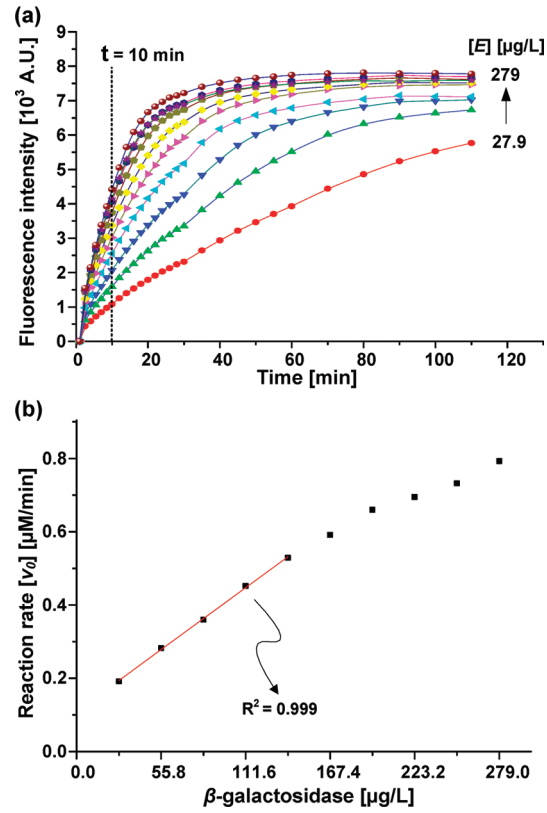

Figure 3. The relationship between the enzyme concentration and the reaction rate. (a) Time courses of the enzyme reactions. The concentrations of β-galactosidase ranged from 27.9 to 279 μg/L with an increment of 27.9 μg/L. (b) The reaction rate versus the enzyme concentration.

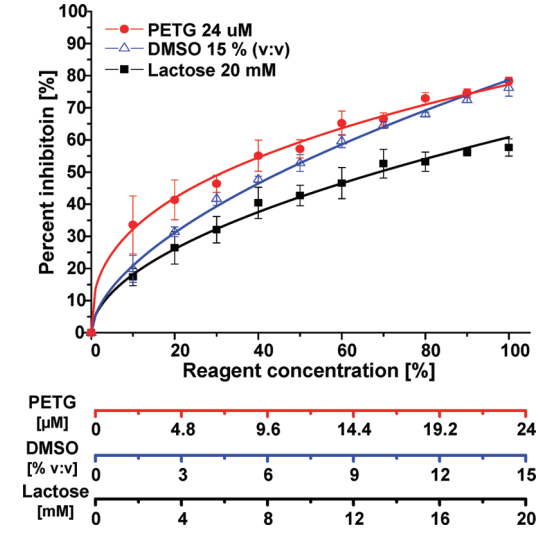

Figure 4. Effect of the inhibitor concentration on enzyme activity. 0∼24 μM of PETG, 20 mM of lactose, and 0∼15% of DMSO (v:v) were used. For this reaction, a constant concentration of the substrate and the enzyme, 133 μM of resorufin-β-D-galactopyranoside and 83.7 μg/L of β-galactosidase, was used.

Figure 4 shows the variations in enzyme activity as the inhibitor concentrations increased. We determined the inhibitor concentration showed 50% inhibition, IC_{50}, for each inhibitor. We obtained half-maximal inhibitory concentrations of PETG and lactose through fitting the concentration response by using the

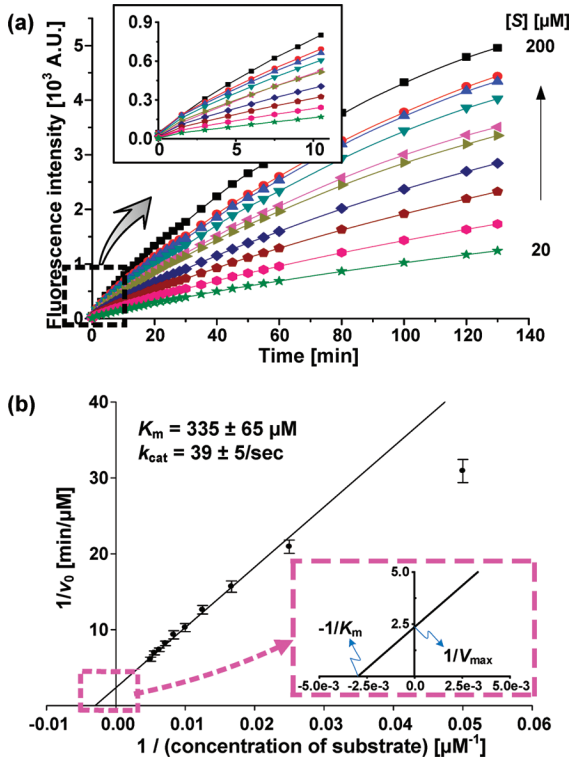

Figure 5. Parallel reactions with a series of substrate concentrations from 20 to 200 μM with an increment of 20 μM. (a) Fluorescent intensity of the product according to the increase of the substrate concentration of β-galactosidase. (b) Lineweaver–Burk reciprocal plot; K_m and k_{cat} were found to be 335 ± 65 μM and 39 ± 5/s, respectively.

modified Michaelis–Menten eq 1. The IC_{50} of PETG and lactose obtained from our on-chip experiment was 10 ± 1.3 μM and 5.3 ± 0.7 mM, respectively. These values compared well with the value of 7.2 μM and 4.2 mM reported in literature, which were determined by using a simple channel network and an electrokinetic flow as a driving force.[5] DMSO is a common solvent used to prepare a concentrated stock solution for high concentrations of inhibitors and substrates. DMSO, in fact, reduces enzyme stability in high concentrations and decreases the reaction rate.[21] Hence, we evaluated the effect of DMSO on enzyme activity. For this, a concentration gradient of DMSO ranging from 1.5% to 15% (v:v) in the enzyme reaction mixture was formed on a chip. We confirmed that 6 ± 0.6% (v:v) of DMSO reduced 50% of enzyme activity from the concentration response curve.

Determination of Reaction Kinetic Parameters. To determine K_m and k_{cat} on a chip, we measured v_0 with a series of substrate concentration changes, 20–200 μM of resorufin-β-D-galactopyranoside, which was produced by introducing 333.3 μM of substrate and assay buffer into reagent inlet ports 1 and 2, respectively. We used 83.7 μg/L of β-galactosidase in the final concentration for each reaction. Figure 5a shows the time courses of the product formation, in which we observed that the enzyme reactions did not reach a plateau in 130 min of reaction time. The fluorescent intensity increased as the substrate concentration increased. We plotted the initial rate on the Lineweaver–Burk reciprocal plot, i.e., a plot of $1/v_0$ as a function of 1/[S], and used linear regression analysis to find the y-intercept ($1/V_{max}$) and the slope (K_m/V_{max}),[22] as shown in Figure 5b. The average K_m in three independent off-chip experiments was 335 ± 65 μM, and the turnover number, k_{cat}, was 39 ± 5/s, as calculated from eq 3. The values of K_m and k_{cat} obtained from our conventional off-chip experiments were 336 ± 75 μM for K_m and 49 ± 9/s for k_{cat}. We compared the on-chip results to the off-chip results and found that the deviation was less than 0.3% for K_m and 20.4% for k_{cat}. Since we carry out the experiments with an enzyme that is a biological sample having variable properties, those deviations can never be entirely eliminated.[22] When we consider these points, the deviations between our on-chip and off-chip experiments were small enough to show the consistency in our experiments. Those small deviations were the most important evidence to verify that the presented microfluidic device can be used to determine the enzyme kinetic parameters in a reliable manner. We also compared the previously reported off-chip results of 550 ± 200 μM for K_m and 70 ± 30/s for k_{cat} and on-chip results of 450 ± 200 μM for K_m and 54 ± 20/s for k_{cat}[5] to our on-chip results. We then found the deviations between our result and the reported values of K_m and k_{cat}: 25.5% and 27.8% for the on-chip experiment and 39% and 30% for the off-chip experiment, respectively. The deviation of our results and the published results mentioned above may be attributed to the use of different substrate and the different measurement method. We used the same substrate of resorufin-β-D-galactopyranoside for on-chip and off-chip experiments. Conversely, Hadd et al.[5] adopted different substrate of o-nitrophenyl-β-D-galactopyranoside for their off-chip experiments. Their K_m and k_{cat} values of conventional experiments were derived from absorbance based measurements. In our case, we used the same substrate, resorufin-β-D-galactopyranoside and the fluorescence based measurement method, for both on-chip and off-chip experiments resulting in less than 0.3 and 20.4% deviations in K_m and k_{cat}, respectively. The difference in the results also might be due to our inclusion 0.1% of BSA and 0.05% Tween 20 in the buffer system. However, the values from our experiment and the literature are valid because our results were located in the range of the standard deviations of the reported results. Practically, several factors, such as weighing, degree of freedom, etc., in the course of statistical analysis influenced the resultant values of the kinetic parameters. For example, when a researcher analyzed identical data sets with different weighing methods, the deviations of 13% for K_m and 24% for k_{cat} were reported.[22,23] Unfortunately, because most researchers did not report on the detailed parameters used in the statistical analysis, it is not easy to quantitatively compare the results obtained from different groups. Through the presented research, we proved the reliability and versatility of our microfluidic system. Therefore, we believe this system could be used to determine the kinetic parameters of newly discovered enzymes and to evaluate the potency of the inhibitor.

CONCLUSIONS

We have demonstrated that enzyme kinetic parameters can be obtained by using a microfluidic system that has 11 parallel

(22) Cornish-Bowden, A. *Analysis of Enzyme Kinetic Data*, 1st ed.; Oxford University Press: Oxford, U.K., 1995.
(23) Wilkinson, G. N. *Biochem. J.* **1961**, *80*, 324–332.

multistep processors. Each processor has individual metering, mixing, and incubating components. We used nanoliters of β-galactosidase and its substrate, resorufin-β-D-galactopyranoside, as the model system for enzyme-catalyzed reactions. By changing the reactant concentrations, we observed the change in the reaction rates and determined the key parameters for the enzyme kinetics, K_m and k_{cat}. There are several potential uses for the presented microfluidic system. The chip could be useful for fast and accurate evaluation of the effects of pH, cofactors, ionic strengths, and the ratio of reactants on reactions, etc. The present system could also be applied in enzyme engineering to develop engineered biocatalysts. In addition, by combining several detection techniques, such as electrochemical methods,[24] UV−vis spectrometry,[25] or mass spectrometry,[26] for on-chip quantitative monitoring, we could increase the sample-in and answer-out capability of the microfluidic system to determine the reaction kinetics with various chemical samples, including nonfluorogenic substrates. The microfluidic system is a useful tool in revealing reaction kinetics and can be applied to many screening processes in biotechnology and other "omic" disciplines.

(24) Garcia, C. D.; Henry, C. S. *Anal. Chem.* **2003**, *75*, 4778–4783.
(25) Salimi-Moosavi, H.; Jiang, Y.; Lester, L.; McKinnon, G.; Harrison, D. J. *Electrophoresis* **2000**, *21*, 1291–1299.
(26) Schilling, M.; Nigge, W.; Rudzinski, A.; Neyer, A.; Hergenrder, R. *Lab Chip* **2004**, *4*, 220–224.

ACKNOWLEDGMENT

This research was partially supported by a grant from the Marine Bioprocess Research Center of the Marine Bio 21 Project funded by the Ministry of Land, Transport and Maritime, Republic of Korea.

SUPPORTING INFORMATION AVAILABLE

Additional information as noted in text. This material is available free of charge via the Internet at http://pubs.acs.org.

Received for review October 3, 2008. Accepted December 17, 2008.

AC8020938